Effect of Variations in the Structure of a Polyleucine-Based α-Helical Transmembrane Peptide on Its Interaction with Phosphatidylglycerol Bilayers†

Feng Liu, Ruthven N. A. H. Lewis, Robert S. Hodges, and Ronald N. McElhaney*

Department of Biochemistry, University of Alberta, Edmonton, Alberta, Canada T6G 2H7

Received December 9, 2003; Revised Manuscript Received January 27, 2004

ABSTRACT: High-sensitivity differential scanning calorimetry and Fourier transform infrared spectroscopy were used to study the interaction of a cationic α-helical transmembrane peptide, acetyl-Lys_2-Leu_{24}-Lys_2-amide (L_{24}), and members of the homologous series of anionic *n*-saturated diacyl phosphatidylglycerols (PGs). Analogues of L_{24}, in which the lysine residues were replaced by 2,3-diaminopropionic acid (L_{24}-DAP), or in which a leucine residue at each end of the polyleucine sequence was replaced by a tryptophan ($WL_{22}W$), were also studied to investigate the roles of lysine side-chain snorkeling and aromatic side-chain interactions with the interfacial region of phospholipid bilayers. The gel/liquid-crystalline phase transition temperature of the host PG bilayers is altered by these peptides in a hydrophobic mismatch-dependent manner, as previously found with zwitterionic phosphatidylcholine (PC) bilayers. However, all three peptides reduce the phase transition temperature and enthalpy to a greater extent in anionic PG bilayers than in zwitterionic PC bilayers, with $WL_{22}W$ having the largest effect. All three peptides form very stable α-helices in PG bilayers, but small conformational changes are induced in response to a mismatch between peptide hydrophobic length and gel-state lipid bilayer hydrophobic thickness. Moreover, electrostatic and hydrogen-bonding interactions occur between the terminal lysine residues of L_{24} and L_{24}DAP and the polar headgroups of PG bilayers. However, such interactions were not observed in PG/$WL_{22}W$ bilayers, suggesting that the cation−π interactions between the tryptophan and lysine residues predominate. These results indicate that the lipid−peptide interactions are affected not only by the hydrophobic mismatch between these peptides and the host lipid bilayer, but also by the tryptophan-modulated electrostatic and hydrogen-bonding interactions between the positively charged lysine residues at the termini of these peptides and the negatively charged polar headgroups of the PG bilayers.

Although about one-third of all proteins are integral membrane proteins, relatively little is known about the detailed structures of membrane proteins (*1*). To date, only 76 unique membrane protein structures have been reported (*2*), compared with the huge number (over 14 000) of soluble proteins in the Protein Data Bank. Most of these integral membrane proteins are composed of tightly packed bundles of transmembrane α-helices that contain about 20 hydrophobic amino acid residues. Statistical analysis shows that the hydrophobic core of these transmembrane α-helices is normally flanked by aromatic residues such as tryptophan or tyrosine and that positively charged lysine or arginine residues are found adjacent to these aromatic residues (*3*). In addition, the orientation of transmembrane proteins obeys the positive-inside rule, that is, the hydrophilic loops rich in positive charges are predominantly located in the cytoplasm. Moreover, although the majority of the phospholipids in cell membranes are zwitterionic or uncharged, phospholipids possessing a negative charge are also present (*4*). Phosphatidylserine is usually the major anionic lipid found in the inner surface of the eukaryotic cell membranes, whereas phosphatidylglycerol is the predominant anionic lipid found in prokaryotic membranes (*5*, *6*). Thus, elucidating the nature of the interactions between integral transmembrane proteins and anionic phospholipids is important for an understanding of the structure and function of membrane proteins. Indeed, many studies have shown that some membrane-associated enzymes and transporters have a requirement for specific anionic phospholipids (*7*−*10*). For example, in *Escherichia coli* anionic lipids are necessary for the translocation activity of SecA and for the efficient integration of the leader peptidase (*9*, *10*). In addition, our previous studies have shown that the Na^+-Mg^{2+}-ATPase of *Acholeplasma laidlawii* requires the presence of an optimal amount of anionic phospholipid for maximal activity, while high levels of anionic phospholipid inhibit activity and may even irreversibly denature the protein (*8*).

Because most transmembrane proteins are relatively large, multidomain macromolecules of complex and often unknown three-dimensional structure and topology that can interact with lipid bilayers in complex, multifaceted ways (*11*−*13*), our understanding of the physical principles underlying lipid−protein interactions remains incomplete, and the actual molecular mechanisms whereby associated lipids could alter the activity, and presumably also the structure and dynamics, of integral membrane proteins are largely unknown. To overcome this problem, a number of workers have designed

† Supported by operating grants from the Natural Sciences and Engineering Research Council of Canada and the Canadian Institutes of Health Research (R.N.M.), and by major equipment grants from the Alberta Heritage Foundation for Medical Research (R.N.M.).

* Corresponding author: Telephone (780) 492-2413. Fax: (780) 492-0095. E-mail: rmcelhan@ualberta.ca.

10.1021/bi036214l CCC: $27.50
Published on Web 03/02/2004

and synthesized peptide models of specific regions of natural membrane proteins and have studied their interactions with model membranes of defined lipid composition (*14*). The synthetic peptide acetyl-K_2-G-L_{24}-K_2-A-amide (P_{24})[1] and its analogues have been successfully utilized as a model of the hydrophobic transmembrane α-helical segments of integral membrane proteins (*14*, *15*). These peptides contain a long sequence of hydrophobic leucine residues capped at both the N- and C-termini with two positively charged, relatively polar lysine residues. Moreover, the normally positively charged N-terminus and the negatively charged C-terminus are blocked to provide a symmetrical tetracationic peptide that will more faithfully mimic the transbilayer region of natural membrane proteins. The central polyleucine region of these peptides was designed to form a maximally stable α-helix, particularly in the hydrophobic environment of the lipid bilayer core, while the dilysine caps were designed to anchor the ends of these peptides to the polar surface of the lipid bilayer and to inhibit the lateral aggregation of these peptides. In fact, CD (*14*) and FTIR (*16*−*18*) spectroscopic studies of P_{24} have shown that it adopts a very stable α-helical conformation both in solution and in lipid bilayers, and X-ray diffraction (*19*), fluorescence quenching (*20*), and FTIR spectroscopic (*16*−*18*) studies have confirmed that P_{24} and its analogues assume a transbilayer orientation with the N- and C-termini exposed to the aqueous environment and the hydrophobic polyleucine core embedded in the hydrocarbon core of the lipid bilayer when reconstituted with various PCs. DSC (*21*−*23*) and ^{2}H NMR spectroscopy (*21*, *22*) studies have shown that P_{24} broadens the L_β/L_α phase transition of the host phospholipid bilayer and reduces its enthalpy. The T_m is shifted either upward or downward, depending on the degree of mismatch between the hydrophobic length of the peptide and the hydrophobic thickness of PC lipid bilayers (*17*), but this shift is not observed in PE bilayers, where P_{24} substantially decreases the T_m in a hydrocarbon chain length-independent manner (*23*). As well, small distortions of the α-helical conformation of P_{24} are also observed in response to peptide−lipid hydrophobic mismatch (*17*). ^{2}H NMR (*24*) and ESR (*25*, *26*) spectroscopic studies have shown that the rotational diffusion of P_{24} about its long axis perpendicular to the membrane plane is rapid in the L_α state of the bilayer and that the closely related peptides L_{24} and $(LA)_{12}$ exist at least primarily as monomers in L_α POPC bilayers, even at relatively high peptide concentrations.

We have previously used three analogues of P_{24}, Ac-K_2-L_{24}-K_2-amide (L_{24}), Ac-DAP_2-L_{24}-DAP_2-amide (L_{24}DAP, DAP is diaminopropionic acid), and Ac-K_2-W-L_{22}-W-K_2-amide ($WL_{22}W$) to study the roles of tryptophan and lysine residues in membrane−protein interactions in zwitterionic PC bilayers (*27*, *28*). First, with the peptide L_{24}DAP, the two pairs of capping lysine residues at the N- and C-termini of L_{24} have been replaced with the lysine analogues DAP, in which three of the four side-chain methylene groups have been removed. This peptide was used to test the so-called snorkel model first suggested by Segrest et al. (*29*) to explain the behavior of positively charged residues in the amphipathic helices present at the surfaces of blood lipoproteins and later extended to transmembrane α-helices by von Heijne et al. (*30*). According to the transmembrane peptide version of the snorkel model, the long, flexible hydrophobic side-chains of lysine or arginine residues could extend along the transmembrane helix so that the terminal charged moiety can reside in the lipid polar headgroup region, while the α-carbon of the amino acid residue remains well below (or possibly above) the membrane−water interface, even when the hydrophobic length of the peptide is considerably different from that of the host lipid bilayer. Because of the shorter spacer arms between the charged amino group and the α-carbon in DAP, L_{24}DAP is expected to be less accommodating to the hydrophobic mismatch between the peptides and the lipids, and any effects of such mismatch on the thermotropic phase behavior of the host lipid bilayer should thus be exaggerated. Second, with the peptide $WL_{22}W$, the residues Leu-3 and Leu-26 of L_{24} are replaced with tryptophans. The preference of aromatic tryptophan or tyrosine residues for the membrane polar/apolar interface has been found to be one of the common features of natural membrane proteins (*31*). Recent studies with WALP peptides (model peptides with two tryptophans at each terminus anchor) have suggested that the interfacial anchoring properties of tryptophan residues in transmembrane peptides can dominate over hydrophobic match effects in the peptide−lipid interactions since the tryptophan indole ring was consistently found to be located near the lipid carbonyl region, regardless of the condition of hydrophobic mismatch between the peptide and the lipid (*32*). Since tryptophan residues have been proposed to anchor the ends of α-helical transmembrane peptides to the polar/apolar interface of the lipid bilayer, we would also expect that $WL_{22}W$ would be less accommodating to hydrophobic mismatch between the peptides and host lipid bilayer than would L_{24}.

To further clarify the role of interfacially localized tryptophan and lysine residues in lipid−protein interactions, we have used DSC and FTIR spectroscopy to study the interactions of L_{24}, L_{24}DAP, and $WL_{22}W$ with a series of anionic PGs with different hydrocarbon chain lengths and have compared these results with those obtained previously for a homologous series of zwitterionic PCs (*28*). Our results demonstrate that the negative charge of the host lipid bilayer has modest but potentially important effects on the electrostatic and hydrogen-bonding interactions between the polar residues at the termini of these peptides and the polar headgroups of the phospholipid. Our results also indicate that the interfacially localized tryptophan residues may play a significant role in the interactions of model peptides with anionic phospholipids, due to its π-electronic structure and/or its strong hydrogen-bonding forming ability.

MATERIALS AND METHODS

The phospholipids used in this study were obtained from Avanti Polar Lipids Inc. (Alabaster, AL) and were used

[1] Abbreviations: P_{24}, acetyl-Lys_2-Gly-Leu_{24}-Lys_2-Ala-amide; L_{24}, acetyl-Lys_2-Leu_{24}-Lys_2-amide; L_{24}DAP, acetyl-DAP_2-Leu_{24}-DAP_2-amide; $WL_{22}W$, acetyl-Lys_2-Trp-Leu_{22}-Trp-Lys_2-amide; $(LA)_{12}$, acetyl-Lys_2-$(Leu\text{-}Ala)_{12}$-Lys_2-amide; DAP, 2,3-diaminopropionic acid; PG, phosphatidylglycerol, where the number before the colon represents the total number of carbon atoms in the hydrocarbon chains and the number after the colon the number of double bonds; DSC, differential scanning calorimetry; FTIR, Fourier transform infrared; L'_β, lamellar gel phase with tilted hydrocarbon chains; L_β, lamellar gel phase with untilted hydrocarbon chains; L_α, lamellar liquid-crystalline phase; T_m, gel/liquid-crystalline phase transition temperature; ΔH, phase transition enthalpy; ΔT, the shift of the T_m of the broad component relative to that of the sharp component.

without further purification. Commercially supplied solvents of at least analytical grade quality were redistilled prior to use. Peptides were synthesized and purified as TFA salts using previously published solid-phase synthesis and reversed phase high-performance liquid chromatographic procedures (*33*).

Samples were prepared for DSC as follows. Lipids and peptides were codissolved in methanol to attain the desired lipid-to-peptide ratio, and the solvent was removed with a stream of nitrogen, leaving a thin film on the sides of a clean glass test tube. This film was subsequently dried in vacuo overnight to ensure removal of the last traces of solvent. Samples containing 0.5−0.8 mg of lipid were then hydrated by vigorous vortexing with a buffer (50 mM Tris, 150 mM NaCl, 1 mM NaN_3, pH 7.4) at temperatures some 10−15 °C above the gel/liquid-crystalline phase transition temperature of the lipid. DSC thermograms were obtained from 0.5-mL samples with a high-sensitivity Microcal VP-DSC instrument (Microcal Inc., Northampton, MA), operating at heating and cooling rates of 10 °C/h. The data were analyzed and plotted with the Origin software package (OriginLab Corporation, Northampton, MA).

Peptide samples to be used in FTIR spectroscopic experiments were converted to the hydrochloride salt by two cycles of lyophylization from 10 mM hydrochloric acid. This procedure was necessary because the trifluoroacetate ion gives rise to a strong absorption band (~1670 cm^{-1}), which partially overlaps the amide I absorption band of the peptide (*17*). Typically, samples were prepared by codissolving lipid and peptide in methanol at a lipid-to-peptide ratios near 30:1 (mol/mol). After removal of the solvent and drying of the film (see above), samples containing 2−3 mg of lipid were hydrated by vigorous mixing with 75 μL of a D_2O-based buffer (50 mM Tris, 150 mM NaCl, 1 mM NaN_3, pD 7.4). The dispersion obtained was then squeezed between the CaF_2 windows of a heatable, demountable liquid cell (NSG Precision Cells, Farmingdale, NY) equipped with a 25 μm Teflon spacer. Once the sample was mounted in the sample holder of the spectrometer, the sample temperature could be varied between 0 and 90 °C by an external, computer-controlled water bath. Infrared spectra were acquired as a function of temperature with a Digilab FTS-40 Fourier transform spectrometer (Bio-Rad, Digilab Division, Cambridge, MA) using data acquisition parameters similar to those described by Mantsch et al. (*34*). The experiment involved a sequential series of 2 °C temperature ramps with a 20-min inter-ramp delay for thermal equilibration, and was equivalent to a scanning rate of 4 °C/h. Spectra were analyzed with software supplied by the instrument manufacturers and other programs obtained from the National Research Council of Canada.

RESULTS

Thermotropic Phase Behavior of PG Bilayers in the Absence of Peptides. As illustrated in Figure 1, in the absence of peptides, the DSC thermograms of the four *n*-saturated diacyl PGs studied exhibit two structurally distinct thermotropic phase transitions. The higher temperature main phase transition is highly energetic and more cooperative. It is also freely reversible, as shown by the absence of significant cooling hysteresis (data not presented). In addition, the

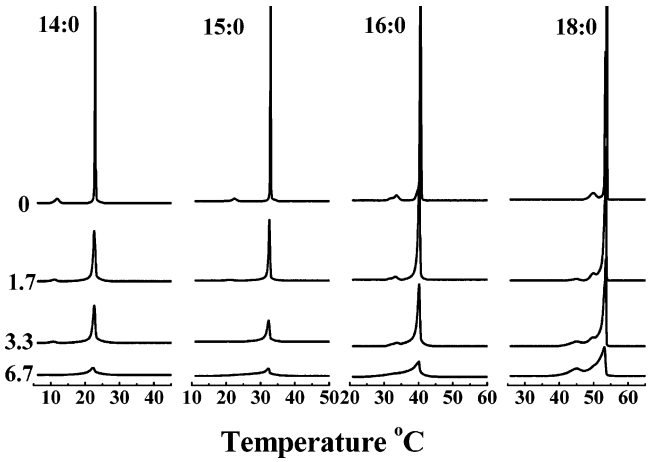

FIGURE 1: Effect of L_{24} on the DSC thermograms of a series of *n*-saturated diacyl-PGs. Thermograms are shown as a function of the acyl chain length (*N*:0) of the lipids, and the mole percent of peptide present in each sample is indicated in the column of numbers printed on the left side of the figure.

temperature of the main phase transitions of these PGs increases smoothly but nonlinearly, and the ΔH's increase linearly, with an increase in hydrocarbon chain length. All these thermodynamic properties are comparable to those reported previously by aqueous dispersions of various *n*-saturated PGs (*35*) and are also similar to those of the rippled gel to liquid-crystalline (P'_β/L_α) phase transitions of comparable *n*-saturated PCs (*17*, *28*).

The lower temperature transition is less cooperative and much less energetic and exhibits a modest cooling hysteresis (Figure 1). The midpoint temperature of this transition also increases with an increase in hydrocarbon chain length. However, the lower temperature transition exhibits a steeper dependence on hydrocarbon chain length so that the interval between it and the main phase transition decreases with increases in the hydrocarbon chain length. These properties are similar to those of the well-defined pretransitions of the *n*-saturated 1,2-dicayl PCs. We therefore suggest that the lower temperature transitions of PGs are L'_β/P'_β phase transitions, similar to those exhibited by the corresponding diacyl PCs. This suggestion should be regarded as tentative, however, until further structural studies such as X-ray diffraction are performed.

The Effect of Peptide Incorporation on the Pretransition. The incorporation of increasing quantities of L_{24} into *n*-saturated dicyl PG bilayers slightly lowers the T_m and significantly lowers the ΔH and cooperativity of the pretransition in all cases. In addition, the pretransition is completely abolished at the highest peptide concentration examined (6.7 mol %) (see Figure 1). It is interesting that the incorporation of peptide is as effective in this regard in the shorter chain PGs as in longer chain PGs. In contrast, the incorporation of P_{24} and L_{24} is more effective in abolishing the pretransition in shorter chain PC bilayers (*17*, *28*). Essentially identical results have been observed for the L_{24} analogues L_{24}DAP and $WL_{22}W$ (data not presented). These findings suggest that the presence of these model peptides may abolish hydrocarbon chain tilt in gel-phase PG bilayers, causing the progressive replacement of the L'_β and P'_β phases with a disordered L_β-like phase with untilted hydrocarbon chains, as observed previously in PC bilayers (*17*, *28*, *36*).

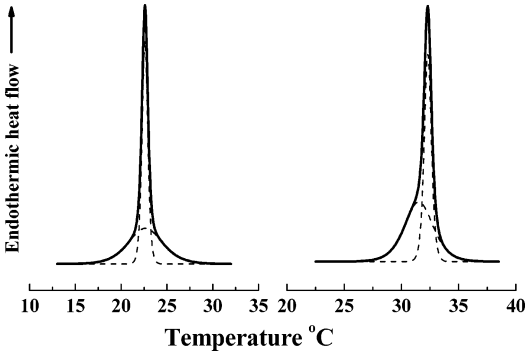

FIGURE 2: Illustration of the curve-fitting procedure used to resolve the components of the DSC heating thermograms. The examples shown are L_{24}/14:0 PG (left panel) and L_{24}/15:0PG (right panel). Both samples contained 3.3 mol % L_{24}.

The Effect of Peptide Incorporation on the Main Transition. The effects of the incorporation of L_{24} on the main phase transitions of the four PGs studied here are also illustrated in Figure 1. In all cases, the incorporation of increasing quantities of peptide produces a two-component DSC endotherm (see Figure 2), as well as a progressive decrease in the ΔH and cooperativity of the overall L_β/L_α phase transition of the host PG bilayer. The relative contribution of the sharp component of the DSC endotherm, which initially possesses a T_m, ΔH, and cooperativity similar to that of the PG alone, decreases in magnitude as the proportion of L_{24} increases. In contrast, the relative contribution of the broad component increases as the peptide concentration increases, and it is the predominant component present at the highest peptide concentration tested. Using the rationale provided in our previous DSC studies of the interaction of P_{24} and related peptides with lipid bilayers (*17*, *28*, *36*), we assign the sharp and broad component of our DSC endotherms to the L_β/L_α phase transitions of peptide-poor and peptide-rich PG domains, respectively. We also observe a small decrease in the temperature and cooperativity of the sharp component of the DSC endotherms. This is ascribed to domain boundary effects arising from the decreasing size of the peptide-poor PG domains, which also explains their progressively smaller ΔH as peptide concentration increases. Note that these characteristic effects of L_{24} and its analogues on the sharp component of the DSC endotherms are noted in all the PGs studied and are hydrocarbon chain length and peptide structure independent.

The effects of peptide incorporation on the thermodynamic parameters of the peptide-rich PG domain, however, do depend on the hydrocarbon chain length and thus on the thickness of the host PG bilayer. For example, as shown in Figure 3, the T_m of the broad component of the DSC endotherm occurs at the same temperature as that of the sharp component in 14:0 PG bilayers, but at progressively lower temperatures in 15:0, 16:0, and 18:0 PG bilayers. If the same trend continues, the T_m of the broad component of the DSC endotherm would occur at a higher temperature than that of the sharp component in 13:0 or shorter chain PG bilayers, as observed previously in PC bilayers (*17*, *28*). Furthermore, in all cases the T_m's of both components decrease with increasing peptide concentration. It is interesting that the phase transition temperatures of the broad and sharp components are almost equal in 14:0 PG but in 15:0 PC bilayers (*17*, *28*). This difference in behavior is likely due to the greater depression of the T_m in PG bilayers compared to PC bilayers produced by the incorporation of comparable amounts of these peptides.

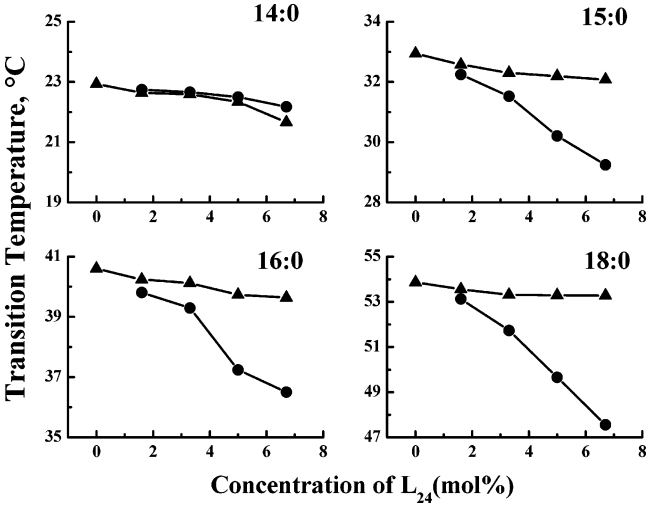

FIGURE 3: Effects of L_{24} concentration on the peak temperatures of the two components of the DSC thermograms exhibited by the mixtures of L_{24} and the *n*-saturated diacyl-PGs. The symbols (▲) and (●) represent the sharp and broad components of the DSC endotherms, respectively.

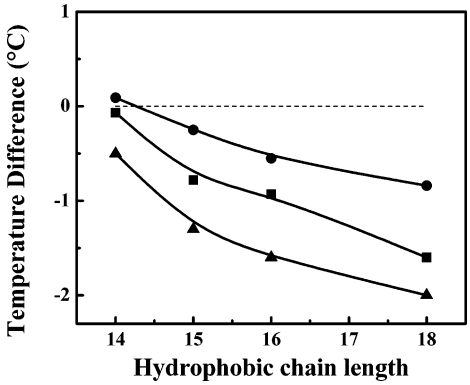

FIGURE 4: Plot of the differences of the transition temperatures of the peptide-associated and the peptide-poor PGs versus the hydrophobic chain length of the lipid bilayer at a peptide concentration of 3.3 mol %. The symbols (▲), (●), and (■) represent peptides $WL_{22}W$, L_{24}DAP, and L_{24}, respectively.

The effects of the lipid hydrocarbon chain length on the shift of the T_m of the broad component relative to that of the sharp component (ΔT) in PG bilayers are presented in Figure 4. With all three model peptides examined, the ΔT of the PG/peptide mixtures becomes larger and more negative with the increase in lipid hydrophobic chain length, which is similar to that reported previously in PC/peptide mixtures with chain lengths of 15 carbons or more (*28*). In addition, we observe that all three model peptides reduce the ΔT of PG bilayers to a greater extent than that of PC bilayers of comparable hydrocarbon chain length. Moreover, in all four PGs examined, $WL_{22}W$ reduces the ΔT to a greater extent than L_{24}, and L_{24} reduces the ΔT to a larger extent than L_{24}-DAP. In PC bilayers, these model peptides also affect the ΔT in a manner dependent on the hydrophobic mismatch between the model peptides and the lipid hydrophobic thickness, but exhibit a different dependence on the structure of these peptides. The differential effects of these peptides on the ΔT of PG and PC bilayers suggest that the thermo-

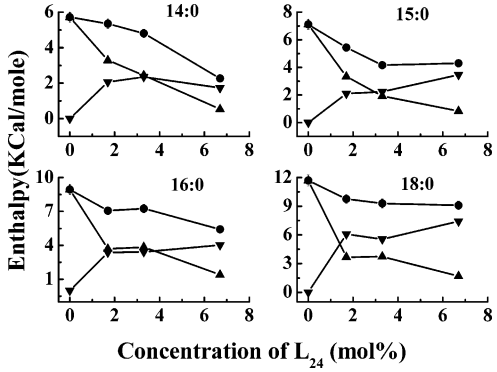

FIGURE 5: Effects of L_{24} concentration on the transition enthalpies of the two components of the DSC thermograms exhibited by mixtures of L_{24} and *n*-saturated diacyl-PGs. The symbols (●), (▲), and (▼) represent the total enthalpy and the enthalpy of the sharp and the broad components of DSC endotherms, respectively.

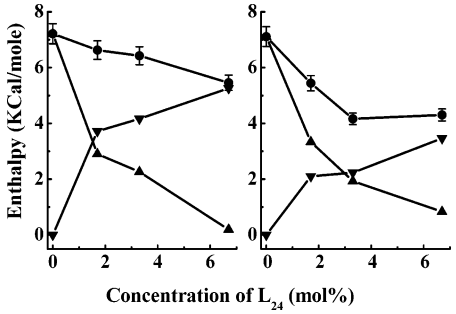

FIGURE 6: Comparison of the effects of L_{24} concentration on the transition enthalpies of L_{24}/15:0 PG mixture (right panel) with that on the transition enthalpies of L_{24}/15:0 PC mixture (left panel). The symbols (●), (▲), and (▼) represent the total enthalpy and the enthalpy of the sharp and the broad components of DSC endotherms, respectively.

tropic phase behavior of peptide/lipid mixtures is influenced by other forces besides those arising from hydrophobic mismatch between the model peptides and the host phospholipid bilayers. A possible molecular mechanism for rationalizing these results will be presented later.

The effect of peptide incorporation on the ΔH's of the four PG bilayers studied here is shown in Figure 5. In all cases, the overall ΔH decreases by about 3 kcal/mol with an increase in peptide concentration. However, the ΔH of the broad component of the DSC endotherm initially increases with increasing peptide concentration before leveling off, while the ΔH of the sharp component decreases rapidly but does not become zero even at the highest peptide concentration tested. In contrast, in comparable PC bilayers, the overall ΔH decreases by only about 2 kcal/mol at the highest peptide concentration (Figure 6). Moreover, the ΔH of the broad component decreases at higher peptide concentration after an initial increase, and the ΔH of the sharp component approaches zero at the highest peptide concentration in PC bilayers. Thus, the lower ΔH of the PG as compared to the PC bilayers at higher peptide concentrations is due to the much lower enthalpy of the broad component of the former system. The fact that the ΔH of the sharp component goes to zero at high peptide concentrations in PC but not in PG bilayers suggests that these peptides are not as well dispersed in the latter mixture. However, the fact that the overall ΔH is nevertheless decreased to a greater extent indicates that these peptides disrupt the gel-state

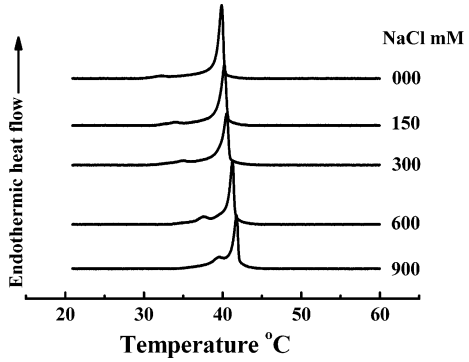

FIGURE 7: Effect of NaCl concentration on the phase behaviors of L_{24}/16:0 PG mixtures at a peptide concentration of 3.3 mol %.

organization to a considerably larger degree in PG as compared to PC bilayers.

To further explore the physical principles underlying PG−peptide interactions, we have examined the effect of salt concentration on the thermotropic phase behavior of 16:0 PG alone and of a L_{24}/16:0 PG mixture containing 3.3 mol % peptide (Figure 7). With an increase of NaCl concentration, there is a gradual increase in the T_m of the main phase transition of the 16:0 PG from 40.1 °C at 0 mM NaCl to 42.1 °C at 900 mM (data not shown). A similar increase is observed in the temperature of the sharp component of the main phase transitions of the L_{24}/16:0 PG mixture, from 39.9 °C at 0 mM NaCl to 41.8 °C at 900 mM NaCl, while a smaller increase was observed in the temperature of the broad component of the main phase transitions of the L_{24}/16:0 PG mixture, from 38.9 °C at 0 mM NaCl to 40.2 °C at 900 mM NaCl. This suggests that the electrical repulsion between the negatively charged phosphate groups in the peptide-enriched domains in PG bilayers is weakened by the presence of these cationic peptides. Moreover, with the increase of the salt concentration, a much larger increase was observed for the temperature of the pretransition of the L_{24}/16:0 PG mixture, from 32.2 °C at 0 mM NaCl to 39.6 °C at 900 mM NaCl, which leads to the overlapping of the pretransition and the main phase transition at 900 mM NaCl. However, the small effects of increases in salt concentration on the T_m, ΔH, and cooperativity of the main phase transition of the L_{24}/16:0 PG mixture suggest that forces other than electrostatic ones play a significant role in the interactions of these model transmembrane peptides with anionic phospholipid bilayers.

Fourier Transform Infrared Spectroscopic Studies of Peptide-Containing PG Bilayers. In these studies, infrared spectra of mixtures of these peptides with each of the four PGs studied were recorded as a function of temperature and as a function of the mole fraction of the peptide. The use of FTIR spectroscopy permits a nonperturbing monitoring of both the structural organization of the lipid bilayer and the conformation of the incorporated peptide. Thus, the changes in the degree of rotational isomeric disorder of the lipid hydrocarbon chains accompanying the L_β/L_α phase transitions of the lipid bilayer can be conveniently monitored by changes in the frequency of the CH_2 symmetric stretching band near 2850 cm^{-1}, changes in gel-state hydrocarbon chain packing by changes in the CH_2 scissoring band near 1468 cm^{-1}, changes in the hydration and/or polarity of the phosphate polar headgroup of the lipid bilayer by changes in the frequency of the O−P−O asymmetrical stretching

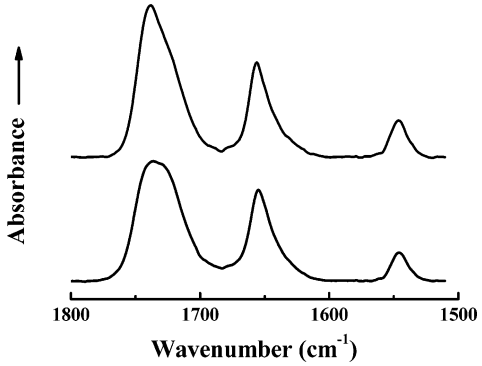

FIGURE 8: FTIR spectra of gel (top) and the liquid-crystalline phase (bottom) formed by a mixture of L_{24} with 16:0 PG at a peptide concentration of 3.3 mol %.

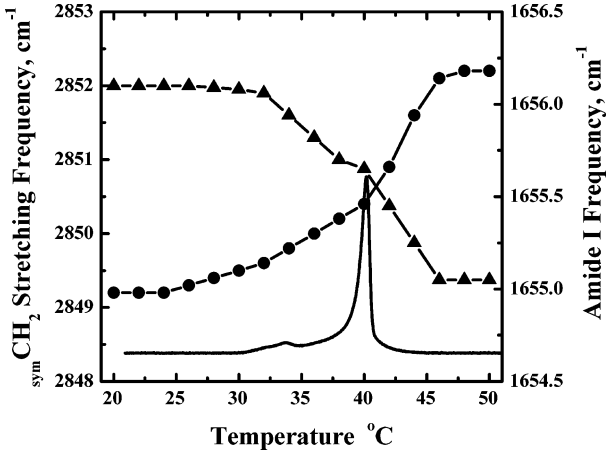

FIGURE 9: Combined plots of CH_2 symmetric stretch (●), peptide amide I band (▲), and calorimetric thermograms as a function of temperature for systems of L_{24}/16:0 PG at a peptide concentration of 3.3 mol %.

bands nears 1215 cm^{-1}, and changes in peptide secondary structure can be monitored by changes in the conformationally sensitive amide I band near 1650 cm^{-1} (*37*).

Illustrated in Figure 8 are the FTIR spectra of L_{24}/16:0 PG (3.3 mol % peptide) mixture in the L_β (top) and L_α (bottom) phases. L_{24} exhibits a sharp band at about 1654 cm^{-1}, indicating that this peptide adopts a predominantly α-helical structure in both phases. A similar sharp amide I band was observed for all three model peptides in all four PGs examined. These results indicate that the potentially stronger electrostatic and hydrogen-bonding interactions between the model peptides and the polar headgroups of anionic PG bilayers do not change the peptide conformation dramatically relative to comparable zwitterionic PC−peptide mixtures. In addition, in the L_α phase, the PG broad C═O stretching bands centered near 1738 cm^{-1} contain subcomponents centered near 1741 and 1726 cm^{-1}. Upon cooling of the sample, an increase in the intensity of higher frequency component relative to that of the lower frequency component is observed. Since these two components have been attributed to a differential infrared absorption by free and hydrogen-bonded ester carbonyl groups, respectively (*34*, *38*, *39*), this observation indicates a loss of water from this region of the bilayer upon entering the L_β state.

Illustrated in Figure 9 are the temperature-dependent changes in the frequencies of the peptide amide I absorption band and the CH_2 symmetric stretching band of the lipid

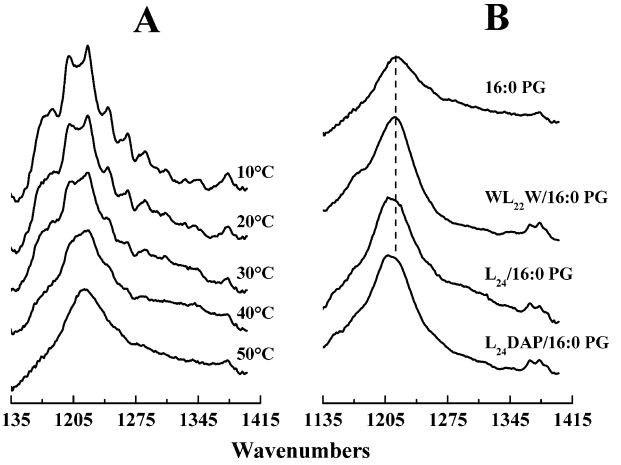

FIGURE 10: (A) The asymmetrical phosphate stretching regions of infrared spectra of 16:0 PG alone in the gel and the liquid-crystalline phases. (B) The asymmetrical phosphate stretching regions of infrared spectra of pure 16:0 PG, L_{24}/16:0 PG, L_{24}DAP/16:0 PG, and $WL_{24}W$/16:0 PG at a peptide concentration of 3.3 mol %. The absorbance spectra shown here were acquired in the liquid-crystalline phase of the lipids.

hydrocarbon chains exhibited by a mixture of L_{24} and 16:0 PG (3.3 mol % peptide). The DSC heating endotherm of this sample is also shown to facilitate a comparison of the calorimetric and FTIR spectroscopic results. The heating endothermic transitions reported by DSC are accompanied by an increase in the CH_2 symmetric stretching frequency, indicating that both the sharp and broad components of the DSC endotherms are associated with lipid hydrocarbon chain-melting events (*17*). Moreover, the lipid phase transition is accompanied by a small decrease in the frequency of the L_{24} amide I band. This frequency change is both reproducible and reversible, suggesting that the conformation of the model peptide is slightly altered by the lipid phase transition. Qualitatively similar results were obtained when the peptides L_{24}DAP and $WL_{22}W$ were incorporated into all four PG bilayers examined here (data not shown). The pattern of the amide I frequency shifts of the model peptide at the gel/liquid-crystalline phase transition of PG bilayers is very similar to that observed when these peptides are incorporated into PC bilayers (*17*, *28*) and thus is also ascribed to small conformational distortions of the peptide helix induced by changes in phospholipid bilayer hydrophobic thickness.

To study the effects of peptide incorporation on the PG polar headgroups in both the L_β and L_α phases, FTIR spectra in the O−P−O asymmetrical stretching region of PG bilayers with and without peptides were obtained at various temperatures. The FTIR spectra of the O−P−O asymmetrical stretching absorption bands of pure 16:0 PG are illustrated in Figure 10A. The strong, relatively broad absorption band centered at 1205 cm^{-1} is the O−P−O asymmetric stretching band and the series of weaker, overlapping bands at 1200, 1222, 1244, 1266, and 1288 cm^{-1} are the CH_2 wagging band progression arising from the gel-state all-trans hydrocarbon chains. With an increase in temperature, the intensity of the CH_2 wagging bands decreases significantly and almost disappears completely upon the gel-to-liquid-crystalline phase transition that occurs around 40 °C. Moreover, above the lipid phase transition, the O−P−O absorption band remains broad, but its maximum frequency shifts to about 1218 cm^{-1}. Similar results were observed for the other three PGs

examined here (data not presented). These observations suggest that in the gel phase the PG phosphate polar headgroups reside in a more polar environment, or are involved in stronger hydrogen-bonding interactions than in the liquid-crystalline phase.

Because of the overlapping of the strong CH_2 wagging band and the O−P−O absorption bands in the gel phase, we will only discuss the effects of the incorporation of model peptides on the O−P−O absorption bands in the L_α phase. Illustrated in Figure 10B are the FTIR spectra of the O−P−O absorption bands of 16:0 PG alone and the mixtures of 16:0 PG with L_{24}, L_{24}DAP or $WL_{22}W$, respectively, in the L_α phase. The O−P−O absorption bands of the mixtures of 16:0 PG with either L_{24} or L_{24}DAP exhibit two components, with one component centered near 1215 cm^{-1}, which is similar to the O−P−O spectra of 16:0 PG alone, and the other centered at a lower frequency of about 1208 cm^{-1}. These observations suggest that some of the phosphate polar headgroups of the PG bilayer reside in more polar environments than others in the presence of these peptides. The lower-frequency population of phospholipids are likely peptide-associated molecules that form more extensive electrostatic and hydrogen-bonding interactions with L_{24} or L_{24}DAP. In contrast, the O−P−O absorption bands exhibited by the mixture of 16:0 PG and $WL_{22}W$ exhibit a one-component spectra centered around 1215 cm^{-1}, which is very similar to that of the pure 16:0 PG. Similar results were obtained with the other PGs studied (data not presented), suggesting that these differences between $WL_{22}W$ and L_{24} or L_{24}DAP are independent of the mismatch between peptide hydrophobic length and lipid hydrophobic thickness. The possible molecular basis for this difference in behaviors between $WL_{22}W$ and L_{24} or L_{24}DAP will be discussed later.

DISCUSSION

In this study, we have shown that model peptides that mimic the hydrophobic transmembrane α-helical segments of integral membrane proteins have somewhat different interactions with anionic PG bilayers than with zwitterionic PC bilayers. In particular, all three model peptides reduce the phase transition temperatures and enthalpies of the PG bilayers to a greater extent than PC bilayers. These results indicate that the nature and strength of the interactions between the somewhat polar and charged amino acid residues at the ends of these model peptides and the polar headgroups of anionic PG and zwitterionic PC bilayers are different.

It is instructive to compare the effects of L_{24} and the closely related peptide P_{24} on the T_m and ΔH of the main phase transitions of zwitterionic PC (*17*, *28*) and PE (*23*, unpublished data) bilayers with that of anionic PG bilayes (this study) of comparable hydrocarbon chain length. As mentioned previously, L_{24} and P_{24} decrease the T_m and ΔH of the main phase transitions of PE bilayers to a greater extent than that of PC bilayers, and the characteristic effects of these peptides on PE bilayers are not as strongly dependent on the bilayer thickness as with PC bilayers. We suggested earlier that the differing effects of peptide incorporation of PE and PC bilayers were due primarily to the stronger lipid polar headgroup interactions in the former system. More specifically, we postulated that the larger effect of transmembrane peptide incorporation on gel-state PE bilayers results from a relatively greater disruption of the intrinsically stronger attractive electrostatic and hydrogen-bonding interactions at the PE bilayer surface as compared to PC bilayers, and that this disruption of attractive interactions between adjacent polar headgroups is sufficiently large to attenuate the effects of hydrophobic mismatch between the peptide and the host lipid bilayer. In the case of anionic PG bilayers, L_{24} incorporation produces a hydrophobic mismatch-dependent decrease in the T_m and ΔH which is less than that observed in PE bilayers but greater than that found in PC bilayers of comparable hydrocarbon chain length. This result is surprising in one sense, in that the binding of water soluble-cationic peptides or proteins to anionic phospholipid bilayers usually produces an increase in T_m and ΔH due to a partial alleviation of the electrostatic repulsion arising from adjacent anionic polar headgroups at the surface of the bilayers, thus stabilizing the gel state (*40*, *41*). The fact that the incorporation of these cationic transmembrane peptides instead actually reduces T_m's of these anionic PG bilayers suggests that their disruption of the attractive hydrogen-bonding network present in gel-state PG bilayers is the dominant effect here. This conclusion is supported by our finding that the thermotropic phase behavior of L_{24}/16:0 PG bilayers is only weakly dependent on variations in salt concentration, which indicates that electrostatic effects are not of primarily importance here. It is interesting to note that the overall effects of L_{24} and P_{24} incorporation are more similar in zwitterionic PC and anionic PG bilayers than in zwitterionic PE bilayers. This suggests that the strength of the electrostatic and hydrogen-bonding interactions between adjacent polar headgroups, rather than polar headgroup charge per se, is the primarily determinant of the effect of the incorporation of these transmembrane peptides on the thermotropic phase behavior of the host phospholipid bilayer.

One purpose of this paper is to study the potential role of the snorkel effect in lipid−peptide interactions by studying the interactions of these model peptides with anionic PG and zwitterionic PC bilayers. The transmembrane version of the snorkel model suggests that the long side-chain of Lys can reach up along the transmembrane helix to allow the terminal charged amino group to reside in the lipid polar headgroup region while the α-carbon of the residue is positioned well below the membrane−water interface. Because of the shorter spacer arms between the charged group and the α-carbon of DAP, the peptide L_{24}DAP is expected to be less accommodating to the hydrophobic mismatch between model peptides and lipid bilayers, and any effects of such mismatch on the thermotropic phase behavior of its host lipid bilayer should be exaggerated. In contrast to this prediction, our previous study actually showed that replacing the terminal Lys residues of L_{24} by DAP attenuates the hydrophobic mismatch effects of the peptide on the thermotropic phase behavior of the host zwitterionic PC bilayer (*28*). This attenuated hydrophobic mismatch effect was rationalized by postulating that the DAP residues are too short to engage in significant electrostatic interactions with the polar headgroups of the host phospholipid bilayer. Therefore, we expect that a differential hydrophobic mismatch effect of L_{24}DAP relative to that of L_{24} will also be observed in PG bilayers, and may be more prominent there because of the potentially stronger electrostatic attractive interactions between these cationic model peptides and the polar headgroups of the

anionic phospholipid. Indeed, our results show that the dependence of the ΔT of PG bilayers on hydrophobic mismatch is less for L_{24}DAP than for L_{24}, as predicted. However, the magnitude of the variation of ΔT with changes in hydrocarbon chain length produced by L_{24} DAP incorporation relative to that by L_{24} is only slightly greater in PG than in PC bilayers, suggesting that the magnitude of the attractive electrostatic interactions between the positively charged lysine or DAP residues at the peptide termini and the negatively charged phosphate groups of PG and PC bilayers are not greatly different.

A comparison of the effects of the incorporation of L_{24} and $WL_{22}W$ on various PG bilayers reveals that the latter peptide produces a slightly greater decrease in the T_m of the broad component of the DSC endotherm than does the former. However, the variations of the difference in temperature between the sharp and broad component with variations in PG hydrocarbon chain length are identical within experimental error for both peptides. Thus, although the presence of tryptophan residues at the ends of the polyleucine core of $WL_{22}W$ perturbs the organization of gel-state PG bilayers slightly, they do not seem to alter the magnitude of the hydrophobic mismatch response between $WL_{22}W$ and the host lipid bilayers, as might be predicted if the tryptophan residues interact strongly with the glycerol backbone region of the PG molecules. A possible reason for these findings will be offered below.

Our current studies also show that L_{24} and L_{24}DAP lower the frequencies of the O−P−O asymmetrical stretching absorption bands of the peptide-associated PGs in the liquid-crystalline phase. Our previous studies have shown that the frequency of the O−P−O asymmetric stretching absorption bands of PGs (1205 cm^{-1} in the L_β phase and 1215 cm^{-1} in the L_α phase) are significantly lower than observed with other phospholipids (1220−1230 cm^{-1}) (*42*), suggesting that the phosphate moieties of the PG molecules are involved in stronger hydrogen-bonding interactions than are other phospholipids. However, our previous studies have shown that the incorporation of model peptides into PC bilayers does not cause any discernible changes in the frequency of the O−P−O asymmetrical stretching absorption bands of the peptide-associated PCs (unpublished data). Taken together, these results suggest that the incorporation of the model peptides L_{24} or L_{24}DAP increase the polarity of the microenvironment of the phosphate group in PG bilayers in the L_α state while having no discernible effect in PC bilayers. Thus, it is possible that the amino groups at both ends of these model peptides are engaged in stronger hydrogen-bonding interactions with the glycerol hydroxyl groups and the phosphate moieties in PG bilayers, or that the model peptides form stronger electrostatic attractions with the negatively charged phosphate moieties in PG than in PC bilayers. The results of our DSC studies, which show only a weak dependence of the thermotropic phase behavior of L_{24}/PG mixtures on salt concentration, would favor the first possibility.

It is interesting to note that the model peptide $WL_{22}W$, in contrast to L_{24} and L_{24}DAP, does not induce any discernible changes in the O−P−O asymmetric stretching absorption bands of PG bilayers in the L_α phase. A possible explanation for the attenuation of the interaction between the lysine residues and the PG phosphate groups is that the tryptophan residues may engage in cation−π interactions with the positively charged side-chains of the lysine residues at the N- and C-termini of $WL_{22}W$. The cation−π interaction is a noncovalent force between a positive charge and the quadrupole moment of an aromatic structure (*43*). Considerable evidence suggests that cation−π interactions are important in many proteins that bind cationic substrates (*44*−*46*). Previous studies of the interactions of four tryptophan analogues with PC bilayers suggested that the preference of tryptophan for the membrane interface is dominated by its π-electronic structure and associated quadrupolar moment (aromaticity) that favor residing in the electrostatically complex interfacial environment (*47*). In the PG/$WL_{22}W$ mixtures, if the positively charged amino groups of the lysine residues form cation−π interactions with the adjacent tryptophan residues, we would expect that these lysine residues would be less likely to form electrostatic attractions with the anionic phosphate group of the PG bilayer. As a result, the model peptide $WL_{22}W$ will have a much smaller effect on the frequency of the O−P−O asymmetrical stretching absorption bands of the peptide-associated PGs in the L_α phase than would L_{24} and L_{24}DAP, as shown by our FTIR results.

In conclusion, the present study and our previous work highlight the importance of the electrostatic and hydrogen-bonding interactions between the lysine residues at the ends of α-helical transmembrane peptides and the polar headgroups of the phospholipids in lipid bilayer membranes. These studies also suggest that specific residues, such as the aromatic tryptophan residues, may modulate such interactions between model peptides and lipid polar headgroups. We hope that further structural and computer modeling investigations will help to further elucidate the molecular basis for these observations.

REFERENCES

1. Kleinschmidt, J. H. (2003) Membrane proteins-introduction. *Cell. Mol. Life Sci. 60*, 1527−1528.
2. White, Stephen. Membrane Proteins of known 3D structure website, University of California, Irvine, http://blanco.biomol.uci.edu/Membrane_Proteins_xtal.html.
3. Killian, J. A., and von Heijne, G. (2000) How proteins adapt to a membrane-water interface. *Trends Biol. Sci. 25*, 429−434.
4. Sandermann, H. (1978) Regulation of membrane enzymes by lipids. *Biochim. Biophys. Acta 515*, 209−237.
5. McElhaney, R. N. (1982) Effects of membrane lipids on transport and enzymic activities in *Current Topics in Membranes and Transport* (Razin, S., and Rottem, S., Eds.) Vol. 17, pp 317−380, Academic Press, New York.
6. McElhaney, R. N. (1985) Membrane lipid fluidity, phase state and membrane function in prokaryotic microorganisms in *Membrane Fluidity in Biology* (Alora, R. A., and Boggs, J. M., Eds.) Vol. 4, pp 147−208, Academic Press, New York.
7. McElhaney, R. N. (1984) The structure and function of the *Acholeplasma laidlawii* plasma membrane. *Biochim. Biophys Acta 779*, 1−42.
8. George, R., Lewis, R. N. A. H., Mahajan, S., and McElhaney, R. N. (1989) Studies on the purified, lipid-reconstituted (Na^++Mg^{2+})-ATPase from *Acholeplasma laidlawii* B membranes: dependence of enzyme activity on lipid headgroup and hydrocarbon chain structure. *J. Biol. Chem. 264*, 11598−11604.
9. Matsumoto, K. (2001) Dispensable nature of phosphatidylglycerol in *Escherichia coli*: dual roles of anionic phospholipids. *Mol. Microbiol. 39*, 1427−1433.
10. van Klompenburg, W., Ridder, A. N., van Raalte, A. L., Killian, J. A., von Heijne, G., and de Kruijff, B. (1997) In vitro membrane integration of leader peptidase depends on the Sec machinery and

anionic phospholipids and can occur posttranslationally. *FEBS Lett. 413*, 109−114.
11. Gennis, R. B. (1989) Membrane dynamics and protein−lipid interactions, in *Biomembranes: Molecular Structure and Function*. Springer-Verlag, pp 166−198, New York.
12. Selinsky, B. S. (1992) Protein−lipid interactions and membrane function, in *The Structure of Biological Membranes* (Yeagle, P., Eds.) pp 603−651, CRC Press, Boca Raton, FL
13. Marsh, D., and Horváth, L. I. (1998) Structure, dynamics and composition of the lipid−protein interface. Perspectives from spin-labeling. *Biochim. Biophys. Acta 1376*, 267−296.
14. Davis, J. H., Clare, D. M., Hodges, R. S., and Bloom, M. (1983) Interaction of a synthetic amphiphilic polypeptide and lipids in a bilayer structure. *Biochemistry 22*, 5298−5305.
15. de Planque, M. R. R., and Killian, J. A. (2003) Protein−lipid interactions studied with designed transmembrane peptides: role of hydrophobic matching and interfacial anchoring. *Mol. Mem. Biol. 20*, 271−284.
16. Zhang, Y.-P., Lewis, R. N. A. H., Hodges, R. S., and McElhaney, R. N. (1992) FTIR spectroscopic studies of the conformation and amide hydrogen exchange of a peptide model of the hydrophobic transmembrane α-helices of membrane proteins. *Biochemistry 31*, 11572−11578.
17. Zhang, Y.-P., Lewis, R. N. A. H., Hodges, R. S., and McElhaney, R. N. (1992) Interaction of a peptide model of a hydrophobic transmembrane α-helical segment of a membrane protein with phosphatidylcholine bilayers: differential scanning calorimetric and FTIR spectroscopic studies. *Biochemistry 31*, 11579−11588.
18. Axelsen, P. H., Kaufman, P. H., McElhaney, R. N., and Lewis, R. N. A. H. (1995) The infrared dichroism of transmembrane helical polypeptides. *Biophys. J. 69*, 2770−2781.
19. Huschilt, J. C., Millman, B. M., and Davis, J. H. (1989) Orientation of alpha-helical peptides in a lipid bilayer. *Biochim Biophys. Acta 979*, 139−141.
20. Bolen, E. J., and Holloway, P. W. (1990) Quenching of tryptophan fluorescence by brominated phospholipid. *Biochemistry 29*, 9638−9643.
21. Huschilt, J. C., Hodges, R. S., and Davis, J. H. (1985) Phase equilibria in an amphiphilic peptide-phospholipid model membrane by deuterium nuclear magnetic resonance difference spectroscopy. *Biochemistry 24*, 1377−1386.
22. Morrow, M. R., Huschilt, J. C., and Davis, J. H. (1985) Simultaneous modeling of phase and calorimetric behavior in an amphiphilic peptide/phospholipid model membrane. *Biochemistry 24*, 5396−5406.
23. Zhang, Y.-P., Lewis, R. N. A. H., Hodges, R. S., and McElhaney, R. N. (1995) Interaction of a peptide model of a hydrophobic transmembrane α-helical segment of a membrane protein with phosphatidylethanolamine bilayers: differential scanning calorimetric and FTIR spectroscopic studies. *Biophys. J. 68*, 847−857.
24. Pauls, K. P., MacKay, A. L., Soderman, O., Bloom, M., Taneja, A. K., and Hodges, R. S. (1985) Dynamic properties of the backbone of an integral membrane polypeptide measured by ^{2}H NMR. *Eur. Biophys. J. 12*, 1−11.
25. Subczynski, W. K., Lewis, R. N. A. H., McElhaney, R. N., Hodges, R. S., Hyde, J. S., and Kusumi, A. (1998) Molecular organization and dynamics of 1-palmitoyl-2-oleoyl-phosphatidylcholine bilayers containing a transmembrane α-helical peptide. *Biochemistry 37*, 3156−3164.
26. Subczynski, W. K., Pasenkiewicz-Gierula, McElhaney, R. N, Hyde, J. S., and Kusumi, A. (2003) Molecular organization and dynamics of 1-palmitoyl-2-oleoyl phosphatidylcholine bilayer membranes containing a transmembrane α-helical peptide with hydrophobic surface roughness. *Biochemistry 42*, 3939−3948.
27. Liu, F., Lewis, R. N. A. H., Hodges, R. S., and McElhaney, R. N. (2001) A differential scanning calorimetric and ^{31}P NMR spectroscopic study of the effect of transmembrane α-helical peptides on the lamellar/reversed hexagonal phase transition of phosphatidylethanolamine model membranes. *Biochemistry 40*, 760−768.
28. Liu, F., Lewis, R. N. A. H., Hodges, R. S., and McElhaney, R. N. (2002). Effect of variations in the structure of a polyleucine-based α-helical transmembrane peptide on its interaction with phosphatidylcholine bilayers. *Biochemistry 41*, 9197−9207.
29. Segrest, J. P., De Loof, H., Dohlman, J. G., Brouillette, C. G., and Anantharamaiah, G. M. (1990) Amphipathic helix motif: classes and properties. *Proteins: Struct. Funct. Genet. 8*, 103−117.
30. Monne, M., Nilsson, I., Johansson, M., Elmhed, N., and van Heijne, G. (1998) Positively and negatively charged residues have different effects on the position in the membrane of a model transmembrane helix. *J. Mol. Biol. 284*, 1177−1183.
31. von Heijne, G. (1994) Membrane proteins: from sequence to structure. *Annu. Rev. Biophys. Biomol. Struct. 23*, 167−192.
32. de Planque, M. R. R., Bonev, B. B., Demmers, J. A. A., Greathouse, D. V., Koeppe, R. E., II, Separovic, F., Watts, A., and Killian, J. A. (2003) Interfacial anchor properties of tryptophan residues in transmembrane peptides can dominate over hydrophobic Matching effects in peptide-lipid interactions. *Biochemistry 42*, 5341−5348.
33. Zhang, Y.-P., Lewis, R. N. A. H., Henry, G. D., Sykes, B. D., Hodges, R. S., and McElhaney, R. N. (1995) Peptide models of helical hydrophobic transmembrane segments of membrane proteins. I. Studies of the conformation, intrabilayer orientation and amide hydrogen exchangeability of Ac-K_2-$(LA)_{12}$-K_2 amide. *Biochemistry 34*, 2348−2361.
34. Mantsch, H. H., Madec, C., Lewis, R. N. A. H., and McElhaney, R. N. (1985) The thermotropic phase behaviour of model membranes composed of phosphatidylcholines containing iso-branched fatty acids. II. Infrared and ^{31}P NMR spectroscopic studies. *Biochemistry 24*, 2440−2446.
35. Zhang, Y.-P., Lewis, R. N. A. H., and McElhaney, R. N. (1997) Calorimetric and spectroscopic studies of the thermotropic phase behavior of the *n*-saturated 1,2-diacyl-phosphatidylglycerols. *Biophys. J. 72*, 779−793.
36. Zhang, Y.-P., Lewis, R. N. A. H., Henry, Hodges, R. S., and McElhaney, R. N. (1995) Peptide models of helical hydrophobic transmembrane segments of membrane proteins. II. DSC and FTIR spectroscopic studies of the interaction of Ac-K_2-$(LA)_{12}$-K_2-amide with phosphatidylcholine bilayers. *Biochemistry 34*, 2362−2371.
37. Lewis, R. N. A. H., and McElhaney, R. N. (1996) FTIR spectroscopy in the study of hydrated lipids and lipid bilayer membranes in *Infrared Spectroscopy of Biomolecules* (Mantsch, H. H., and Chapman, D., Eds.) pp 159−202, John Wiley and Sons, New York.
38. Blume, A., Hubner, W., and Messner, G. (1988) Fourier transform infrared spectroscopy of ^{13}C═O-labeled phospholipids hydrogen bonding to carbonyl groups. *Biochemistry 27*, 8239−8249.
39. Lewis, R. N. A. H., McElhaney, R. N., Pohle, W., and Mantsch, H. H. (1994) The components of the carbonyl stretching band in the infrared spectra of hydrated 1,2-diacylglycerolipid bilayers: a reevaluation. *Biophys. J. 67*, 2367−2375.
40. McElhaney, R. N. (1986) Differential scanning calorimetric studies of lipid−protein interactions in model membrane systems. *Biochim. Biophys. Acta 864*, 361−421.
41. Lewis, R. N. A. H., and McElhaney, R. N. (1992) The mesomorphic phase behavior of lipids bilayers in *The Structure of Biological Membranes* (Yeagle, P. L., Ed.) pp 73−155, CRC Press, Boca Raton, Florida, 1992.
42. Lewis, R. N. A. H., Pohle, W., and McElhaney, R. N. (1997) The interfacial structure of phospholipid bilayers: Differential scanning calorimetry and Fourier transform infrared spectroscopic studies of 1,2-dipalmitoyl-*sn*-glycero-3-phosphorylcholine and its dialkyl and acyl-alkyl analogues. *Biophys. J. 70*, 2736−2746.
43. Dougherty, D. A. (1996) Cation-π interactions in chemistry and biology: a new view of benzene, Phe, Tyr, and Trp. *Science 271*, 163−168.
44. Sussman, J. L., Harel, M., Frolow, F., Oefner, C., Goldman, A., Toker, L., and Silman, I. (1991) Atomic structure of acetylcholinesterase from *Torpedo californica*: a prototypic acetylcholine-binding protein. *Science 253*, 872−879.
45. Unwin, N. (1993) Nicotinic acetylcholine receptor at 9 Å resolution. *J. Mol. Biol. 229*, 1101−1124.
46. Satin, J., Kyle, J. W., Chen, M., Bell, P., Cribbs, L. L., Fozzard, H. A., and Rogart, R. B. (1992) A mutant of TTX-resistant cardiac sodium channels with TTX-sensitive properties. *Science 256*, 1202−1205.
47. Yau, W.-M., Wimley, W. C., Gawrisch, K., and White, S. H. (1998) The preference of tryptophan for membrane interfaces. *Biochemistry 37*, 14713−14718.

BI036214L